Accumulation of protease-resistant prion protein (PrP) and apoptosis of cerebellar granule cells in transgenic mice expressing a PrP insertional mutation

Roberto Chiesa*, Bettina Drisaldi*, Elena Quaglio*, Antonio Migheli[†], Pedro Piccardo[‡], Bernardino Ghetti[‡], and David A. Harris*[§]

*Department of Cell Biology and Physiology, Washington University School of Medicine, St. Louis, MO 63110; [†]Department of Neuroscience, Laboratory of Neuropathology, University of Turin, 10126 Turin, Italy; and [‡]Division of Neuropathology, Indiana University School of Medicine, Indianapolis, IN 46202

We have generated lines of transgenic mice that express a mutant prion protein (PrP) containing 14 octapeptide repeats whose human homologue is associated with an inherited prion dementia. These mice develop a neurological illness with prominent ataxia at 65 or 240 days of age, depending on whether the transgene array is, respectively, homozygous or hemizygous. Starting from birth, mutant PrP is converted into a protease-resistant and detergent-insoluble form that resembles the scrapie isoform of PrP, and this form accumulates dramatically in many brain regions throughout the lifetime of the mice. As PrP accumulates, there is massive apoptosis of granule cells in the cerebellum. Our analysis provides important insights into the molecular pathogenesis of inherited prion disorders in humans.

Prion diseases are fatal disorders of the central nervous system of both humans and animals that can have an infectious, genetic, or idiopathic origin. The key event in the pathogenesis of all forms of these diseases is the conformational conversion of a normal cell surface glycoprotein [cellular isoform of the prion protein (PrP^C)] into a pathogenic isoform [scrapie isoform of PrP (PrP^{Sc})] that has a high content of β-sheet (1). PrP^{Sc} accumulates in the brains of affected individuals in a detergent-insoluble and protease-resistant form that is likely to be the main component of infectious prion particles. Hereditary prion diseases, which include 10% of the cases of Creutzfeldt-Jakob disease and all cases of Gerstmann-Sträussler syndrome and fatal familial insomnia, are inherited in an autosomal dominant fashion and are linked to point and insertional mutations in the prion protein (PrP) gene on chromosome 20 (2, 3). These mutations are presumed to favor spontaneous conversion of PrP to the PrP^{Sc} state.

We have recently developed a transgenic (Tg) mouse model of a familial prion disease by expressing the mouse PrP homologue of a nine-octapeptide insertional mutation (PG14) described in human patients (4). This insertion is the largest thus far identified in the PrP gene and is associated with a prion disease characterized by progressive dementia and ataxia, and by the presence of PrP-containing amyloid plaques in the cerebellum and basal ganglia (5–7). Tg(PG14) mice develop a slowly progressive neurological disorder characterized clinically by ataxia and neuropathologically by PrP deposition in a synaptic-like pattern, gliosis, and loss of cerebellar granule cells. Moreover, PG14 PrP molecules expressed in the brains of the mice acquire the major biochemical properties of PrP^{Sc}, including partial resistance to proteinase K digestion, insolubility in nondenaturing detergents, and resistance to cleavage of the C-terminal glycolipid anchor by phospholipase. Thus, Tg(PG14) mice recapitulate several of the essential clinical, neuropathological, and biochemical features of inherited human prion diseases.

Although many studies of scrapie in rodents and other hosts have been carried out to understand the pathogenesis of infectiously acquired prion diseases, the absence of a suitable animal model has precluded similar analysis of the familial forms of these disorders. Several other lines of PrP transgenic mice have been described that spontaneously develop a neurological illness (8–11). However, only one of these expresses a mutant PrP (P101L) that is associated with a familial prion disease, and mice of this line do not produce detectable protease-resistant PrP in their brains (12, 13). Several fundamental questions about familial prion diseases therefore remain unexplored, such as the time course of PrP^{Sc} accumulation, the anatomical distribution of PrP^{Sc} production, and the relationship of PrP^{Sc} to the development of clinical symptoms and neuropathology. To address these issues, we undertook a prospective study of Tg(PG14) mice from birth through the terminal phase of their illness using a combined biochemical and histological approach. Our results provide important insights into the natural history and pathogenesis of familial prion diseases.

Materials and Methods

Tg Mice. Production of Tg mice expressing wild-type (WT) and PG14 mouse PrPs tagged with an epitope for the monoclonal antibody 3F4 has been reported previously (4). To monitor the development of neurological symptoms, mice were scored according to a set of objective criteria (4). The experiments reported here were performed on Tg(PG14) mice of the A2 and A3 lines generated by breeding onto either (C57BL/6J × CBA/J/Prn-$p^{+/+}$) or (C57BL/6J × 129/Prn-$p^{0/0}$) backgrounds (4). Since there were no differences in PrP properties between these lines, data from the lines were pooled for the Western blot analyses shown in Figs. 1, 2, and 3A. As controls, we used Tg(WT-E1$^{+/+}$) mice on the (C57BL/6J × 129/Prn-$p^{0/0}$) background.

Biochemical Assays. Assays of detergent-insolubility and proteinase K resistance of PrP in brain were carried out and quantitated as described previously (4). Western blots of samples from Tg mice were developed with monoclonal antibody 3F4 (14), which selectively recognizes PrP encoded by the transgene. PrP from nontransgenic CD1 mice was recognized with polyclonal antibody P45-66 (15). Glial fibrillary acidic protein (GFAP) was recognized with a rabbit polyclonal antibody from Dako and actin with monoclonal antibody C4 (kindly provided by John Cooper).

Histoblotting. Coronal sections (8- μm thick) of unfixed frozen mouse brain were subjected to histoblotting as described elsewhere (16), except that proteinase K was used at a concentration of 0.25 μg/ml at 37°C for 1 h. Membranes were incubated with 3F4 antibody, followed by alkaline phosphatase-conjugated anti-mouse IgG secondary antibody (Jackson Immunoresearch), and were then developed with 5-bromo-4-chloro-3-indolyl phosphate/nitroblue tetrazolium substrate (Sigma).
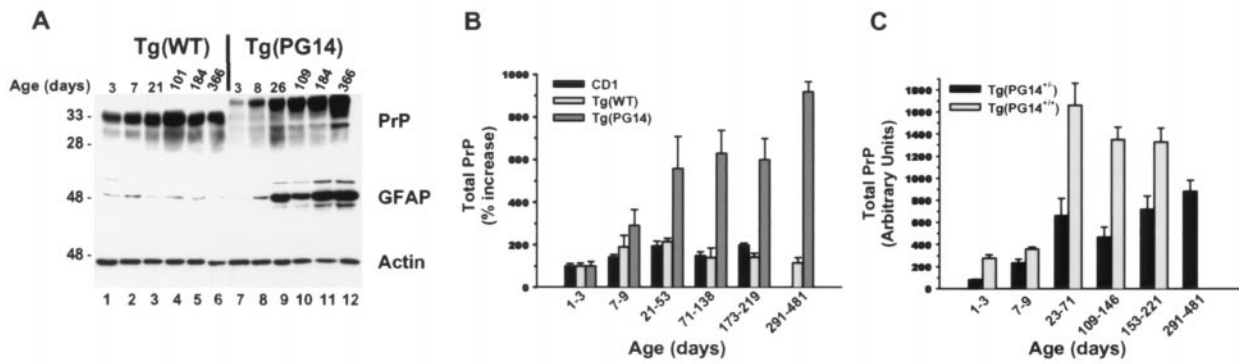

Fig. 1. PG14 PrP accumulates with age in the brains of Tg(PG14) mice. (*A*) Brain extracts of Tg(WT$^{+/+}$) and Tg(PG14$^{+/-}$) mice of the indicated ages were separated by SDS-PAGE, and immunoblotted with antibodies specific for PrP, GFAP, or actin. Each lane represents 10 μg of total protein. (*B*) The amount of PrP in the brains of Tg(WT$^{+/+}$), Tg(PG14$^{+/-}$), and nontransgenic CD1 mice in each age group was quantitated by densitometric analysis of Western blots and was expressed as a percentage of the amount present in 1- to 3-day-old mice. Each bar represents the mean ± SEM of values from three to seven animals. (*C*) The amount of PrP in the brains of Tg(PG14$^{+/-}$) and Tg(PG14$^{+/+}$) mice in each age group was quantitated by densitometric analysis of Western blots and was expressed in arbitrary units. Each bar represents the mean ± SEM of values from three to seven animals. Size markers are given in kDa.

Histology. Preparation of sections and immunohistochemical staining using antibodies to PrP (3F4) and GFAP were carried out as described previously (4). *In situ* end labeling (ISEL) of paraffin-embedded sections was performed as described previously (17).

DNA Laddering. DNA was extracted from cerebella as described by Forloni *et al.* (30) and was subjected to Southern blotting. The blot was probed with *Eco*RI/*Hind*III-digested mouse genomic DNA by using the Gene Images CDP-Star Chemiluminescent Detection System (Amersham Pharmacia).
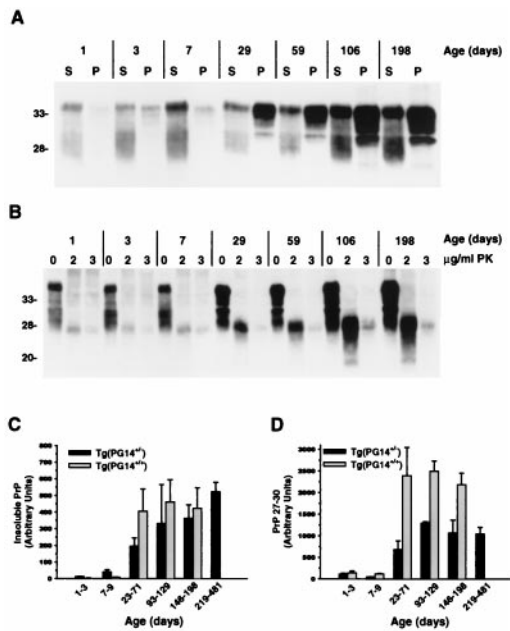

Fig. 2. The amount of detergent-insoluble and protease-resistant PG14 PrP increases with age in the brains of Tg(PG14) mice. (*A*) Brain lysates from Tg(PG14$^{+/+}$) mice of the indicated ages were subjected to ultracentrifugation, and PrP in the supernatants (S lanes) and pellets (P lanes) was analyzed by Western blotting. (*B*) Brain lysates from Tg(PG14$^{+/+}$) mice of the indicated ages were incubated with 0–3 μg of proteinase K (PK) for 30 min at 37°C, and PrP was visualized by Western blotting. The undigested samples (0 μg/ml PK) represent 50 μg of protein, and the other samples represent 200 μg of protein. The protease-resistant fragment (PrP 27-30) migrates between 27 and 30 kDa. (*C*) The amount of PG14 PrP in the pellet fraction after ultracentrifugation (see *A*) was quantitated by densitometric analysis of Western blots of samples from Tg(PG14$^{+/-}$) and Tg(PG14$^{+/+}$) mice. Each bar represents the mean ± SEM of four to eight replicate analyses of samples from four to seven brains. (*D*) The amount of PrP 27-30 that was produced by digestion with 2 μg/ml of proteinase K (see *B*) was quantitated by densitometric analysis of Western blots of samples from Tg(PG14$^{+/-}$) and Tg(PG14$^{+/+}$) mice. Each bar represents the mean ± SEM of four to eight replicate analyses of samples from four to seven brains.
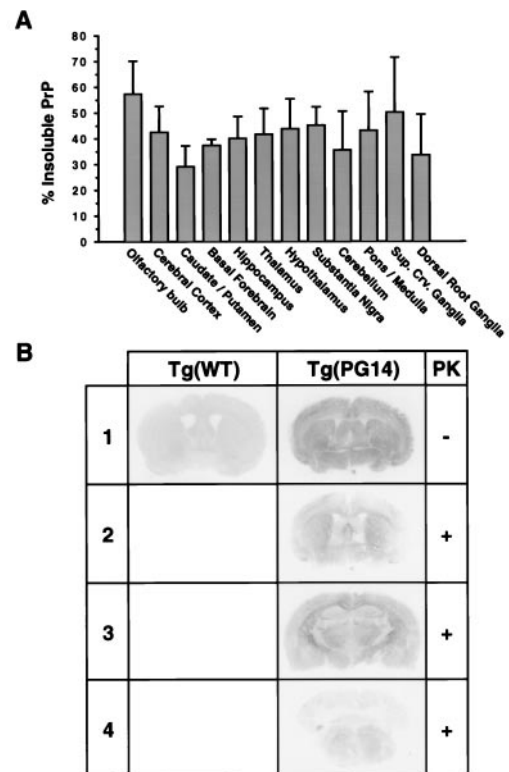
NEUROBIOLOGY

Fig. 3. Protease-resistant and detergent-insoluble PrP are widely distributed in the brains of Tg(PG14) mice. (*A*) Detergent insolubility of PrP from dissected brain regions was analyzed and quantitated as in Fig. 2 *A* and *C*. Each bar represents the mean ± SEM of three to five replicates from four Tg(PG14$^{+/-}$) mice, ranging in age from 79 to 239 days. (*B*) Coronal cryostat sections from the brain of a Tg(WT$^{+/+}$) mouse (182 days old) and a Tg(PG14$^{+/+}$) mouse (192 days old) at the level of the caudate-putamen (rows 1 and 2), thalamus (row 3), and cerebellum (row 4) were subjected to histoblotting, either before (row 1) or after (rows 2–4) treatment with proteinase K.

Table 1. Clinical illness in Tg(PG14) mice

	(C57BL/6J × CBA/J/Prn-p$^{+/+}$)		(C57BL/6J × 129/Prn-p$^{0/0}$)	
	Hemizygous	Homozygous	Hemizygous	Homozygous
Age at onset	235 ± 10 (61)	68 ± 9 (7)	243 ± 7 (76)	64 ± 4 (28)
Age at death	371 ± 21 (42)	115 ± 12 (7)	449 ± 17 (23)	138 ± 10 (27)
Duration of illness	154 ± 14 (35)	49 ± 11 (5)	233 ± 18 (20)	92 ± 9 (19)

Entries show the mean number of days ± SEM. The number of animals in each group is given in parentheses. Hemizygous and homozygous refer to the status of the PG14 transgene array. Data are for mice belonging to the Tg(PG14-A2) and Tg(PG14-A3) lines.

Results

Time Course of the Clinical Illness in Tg(PG14) Mice. We have previously reported that the A2 and A3 lines of Tg(PG14) mice (both of which express mutant PrP at levels similar to that of endogenous PrP) develop a progressive and ultimately fatal neurological disorder characterized by ataxia, kyphosis, foot-clasp reflex, waddling gait, difficulty righting, and weight loss (4). In contrast, Tg(WT) mice from the E1 line that express WT PrP at even higher levels (three to four times endogenous PrP) remain healthy. We have now performed a detailed prospective analysis of the appearance of clinical symptoms in A2 and A3 Tg(PG14) mice.

We observed a profound effect of the zygosity of transgene array on the time course of the disease. On the (C57BL/6J × CBA/J) genetic background that was used to create the founders, mice hemizygous for the transgene array first develop symptoms at 235 days of age, whereas mice homozygous for the transgene array have a disease onset at 68 days of age (Table 1). The duration of the illness is also much shorter in homozygous mice (49 days) than in hemizygous mice (154 days). Since homozygous mice express approximately twice as much PrP as hemizygous mice (see Fig. 1C), these observations indicate that the rate at which the illness progresses is strongly correlated with the expression level of mutant PrP. This conclusion is consistent with our previous finding that the Tg(PG14) B and C lines, which express low levels of the mutant protein (0.15 times the endogenous PrP level), do not develop a neurological disorder within the life span of the animals (4).

In an attempt to ascertain the influence of endogenous WT PrP on the disease characteristics, we also analyzed Tg(PG14) mice that had been bred onto a (C57BL/6J × 129/Prn-p$^{0/0}$) genetic background in which both copies of the PrP gene have been ablated (18) (Table 1). Although the age at disease onset was not significantly different between the two genetic backgrounds, we did observe that the duration of illness was somewhat longer in (C57BL/6J × 129/Prn-p$^{0/0}$) mice (233 days when the transgene array is hemizygous, and 92 days when the transgene array is homozygous). Whether this phenomenon reflects a potentiating effect of endogenous PrP on the disease phenotype or the influence of other genetic loci that differ between the two strains remains to be determined. In a previous publication (4), we reported that the disease progression was accelerated rather than retarded on the (C57BL/6J × 129/Prn-p$^{0/0}$) background, but this conclusion was based on analysis of a very small number of animals.

PG14 PrP Accumulates in the Brains of Tg Mice. To correlate the appearance of clinical symptoms with expression of the mutant protein, we first determined the total amount of PG14 PrP in the brains of mice of different ages using Western blotting. We observed that as Tg(PG14) mice aged, there was a nearly 10-fold increase in the total amount of mutant PrP in their brains (Fig. 1 A and B). This phenomenon was specific for the mutant form of the protein, since the amount of WT PrP in the brains of Tg(WT) and nontransgenic CD1 mice varied by <2-fold over the lifetime of the animals, and the amount of actin remained relatively constant. As expected, the amount of PG14 PrP was about 2-fold higher in Tg(PG14$^{+/+}$) mice than in Tg(PG14$^{+/-}$) mice at all ages (Fig. 1C). To address the possibility that accumulation of PG14 PrP is due to increased gene transcription,

we performed Northern blots to assay PrP mRNA. We found that there was no significant change in the amount of transgenically encoded PrP mRNA during postnatal development of either Tg(PG14) or Tg(WT) mice (data not shown). The vector used to drive transgene expression in both sets of mice incorporates the mouse PrP promoter (19), so that the temporal pattern of transgene expression mirrors that of endogenous PrP.

Mutant PrP Is Converted to a PrP^{Sc}-Like State throughout the Lifetime of Tg(PG14) Mice. To determine whether the mutant PrP that accumulated in the brains of Tg(PG14) mice has the properties of the PrP^{Sc} isoform, we assayed its detergent insolubility by ultracentrifugation and its protease resistance by digestion with low concentrations of proteinase K (1–3 μg/ml). Although PG14 PrP is 10–50 times less protease resistant than some strains of PrP^{Sc} from human and rodent brain, it is cleaved at the same site as authentic PrP^{Sc} to yield a characteristic PrP 27-30 core fragment (4). As shown in Fig. 2, detergent-insoluble and protease-resistant PG14 PrP is already synthesized in the brains of transgenic mice during the first week of life, well before the animals develop clinical symptoms (Table 1) or neuropathological changes (see below). The amount of detergent-insoluble and protease-resistant PrP increased dramatically with age, with levels in the oldest terminally ill animals that were up to 80-fold and 20-fold higher, respectively, than in newborn mice. We noted that PrP^{Sc}-like protein accumulated more rapidly and to higher levels in Tg(PG14$^{+/+}$) mice than in Tg(PG14$^{+/-}$) mice (Fig. 2 C and D), correlating with the accelerated disease progression in the homozygous animals. We also found that the proportion of total PG14 PrP that was detergent insoluble increased from 16.1 ± 5% in neonatal mice to 84.1 ± 2% in terminally ill mice, suggesting that the aggregation state of the protein increased with age. WT PrP in the brains of Tg(WT) mice was detergent soluble and protease sensitive under the conditions of our assays (data not shown; ref. 4).

Protease-Resistant and Detergent-Insoluble PrP Is Widely Distributed in the Brains of Tg(PG14) Mice. To assess the anatomical distribution of PrP^{Sc}-like molecules, we dissected individual brain regions and analyzed them by Western blotting for their content of detergent-insoluble and protease-resistant PG14 PrP, and we also carried out histoblots (16) of cryostat sections of brain. Detergent-insoluble PrP (Fig. 3A) and protease-resistant PrP (data not shown) were found to be widely distributed in the brains of Tg(PG14) mice, with roughly similar amounts present in 10 separate regions; these forms of the protein were also present in superior cervical and dorsal root ganglia. Histoblots of brain sections from terminally ill Tg(PG14) mice revealed protease-resistant PrP in most areas, with particular concentrations in the medial caudate-putamen, septum, corpus callosum, anterior commissure, ventral thalamus, globus pallidus, and hippocampus (Fig. 3B). Consistent with immunohistochemical experiments (see below), the cerebella of terminally ill mice contained less protease-resistant PrP than other regions, probably because of the substantial loss of granule cells that had occurred by this stage. In histoblots from younger animals (25–100 days old), protease-resistant PrP was widely distributed throughout the brain, including in the cerebellum (data not shown). Histoblots of Tg(WT) mice did not show any PrP after proteinase K treatment.
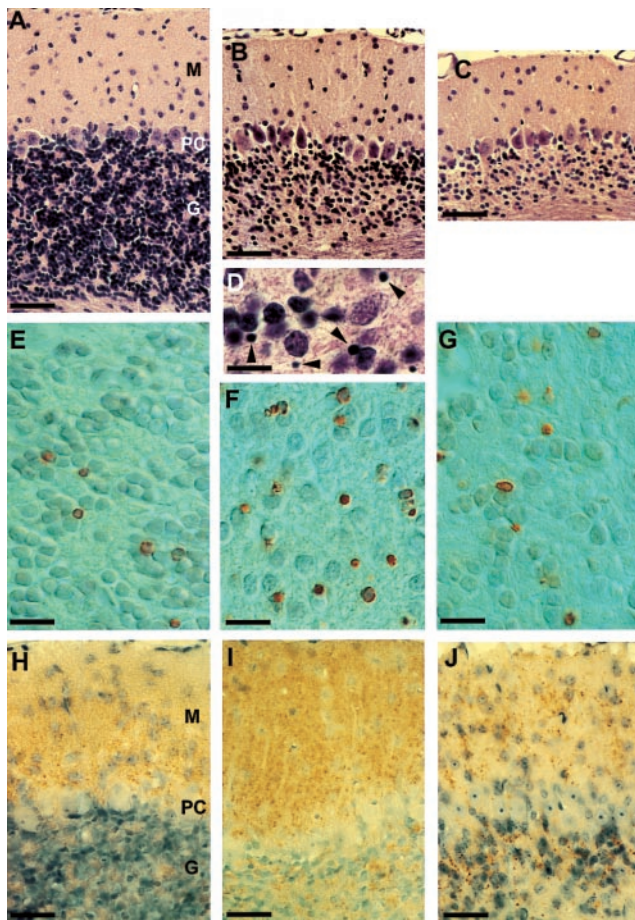
Fig. 4. Neuropathological changes in the cerebella of Tg(PG14⁺/⁺) mice. Hematoxylin and eosin-stained sections showing the cerebellar cortex of mice of 22 days (*A*), 100 days (*B* and *D*), and 183 days (*C*) of age. M, molecular layer; PC, Purkinje cell layer; G, granule cell layer. Note the dramatic decrease in the number of granule cells with age. Arrowheads in *D* indicate pyknotic nuclei. ISEL-stained sections showing positively stained cells (brown) in the granule cell layer from mice of 31 days (*E*), 53 days (*F*), and 181 days (*G*) of age. PrP immunostaining of cerebellar cortex from mice of 22 days (*H*), 100 days (*I*), and 181 days (*J*) of age. Note the small punctate deposits of PrP. Scale bars are: 50 μm (*A*–*C*), 10 μm (*D*), 13 μm (*E*–*G*), 32 μm (*H*–*J*).

Cerebellar Granule Cells of Tg(PG14) Mice Degenerate by an Apoptotic Mechanism.

We previously reported that one of the most noticeable neuropathological abnormalities in Tg(PG14) mice is a massive loss of cerebellar granule cells, which causes severe atrophy of the cerebellum (4). To investigate whether this phenomenon reflects a developmental defect in proliferation of granule cell precursors, or degeneration of cells once they become postmitotic, we analyzed hematoxylin and eosin-stained sections of cerebella from mice of different ages (Fig. 4 *A*–*C* and Table 2). We found that in Tg(PG14) mice granule cells appeared to develop normally, with proliferation in the external granule cell layer, followed by migration to the internal granule cell layer. Although we have not carried out cell counts, the density of granule cells in mice at 7 and 22 days of age did not appear to be markedly different in Tg(PG14⁺/⁺) animals compared with Tg(WT) or nontransgenic animals. In all mice, the external granule cell layer had disappeared by 3 weeks of age, arguing against any gross defect in cell migration. By 41 days of age, however, there was a noticeable decrease in the number of cells in the internal granule cell layer of Tg(PG14⁺/⁺) mice compared with Tg(WT) mice, a difference that became even more marked as the mice aged. By the time the Tg(PG14⁺/⁺) mice were terminally ill (≈180 days), there were almost no granule cells remaining.

Table 2. Pathology in the cerebellar cortex of Tg(PG14⁺/⁺) mice

Age, days	PrP immunostaining*	Granule cell loss	ISEL (granule cell layer)	GFAP immunostaining*
7	0	0	2†	1
22	0	0	1	1
31	1	0	2	2
41	2	1	2	2
53	2	2	4	3
71	4	2	4	4
86	4	3	4	4
100	3	3	4	4
181	2	4	2	4
183	2	4	2	4

Scoring is on a scale of 0 (minimum) to 4 (maximum).
*Staining was present in both the granule cell and molecular layers, but was most prominent in the latter.
†This score reflects cells in the external granule cell layer that undergo developmentally programmed cell death between postnatal days 1 and 14 (20).

Several features demonstrate that granule cell degeneration in Tg(PG14) mice occurred by apoptosis. First, at the peak of granule cell degeneration (50–100 days of age), examination of hematoxylin and eosin-stained sections revealed numerous granule cells with pyknotic and fragmented nuclei (Fig. 4*D*). Second, degenerating neurons were stained positively by the method of ISEL, which reveals DNA fragmentation (Fig. 4 *E*–*G* and Table 2). In Tg(PG14⁺/⁺) mice, a small number of ISEL-positive neurons were first noted in the internal granule cell layer at 22 days of age, at the time when granule cells have just completed their migration. (In younger mice, ISEL-positive neurons were present in the external granule cell layer even in control mice because of the programmed death of granule cells that occurs during this period (20).) The number of ISEL-positive neurons increased dramatically in older animals, reaching a maximum of >20 per high-power ($\times$100) field between 50 and 100 days of age. The number of positively staining neurons declined somewhat thereafter, as the total number of granule cells rapidly diminished. For comparison, Tg(WT) mice never showed more than one to two ISEL-positive neurons in the entire internal granule cell layer. In preliminary experiments, essentially all ISEL-positive neurons in the internal granule cell layer of Tg(PG14) mice were found to stain with an antibody that recognizes activated caspase-3 (data not shown).

Finally, when DNA was extracted from whole cerebella, a characteristic 200-bp ladder, indicative of internucleosomal cleavage, was observed in both the A2 and A3 lines of Tg(PG14) mice, but not in Tg(WT) mice (Fig. 5). Laddering was not observed in DNA extracted from other brain regions (data not shown).

Other Neuropathological Changes in Tg(PG14) Mice.

We previously reported that Tg(PG14) mice display thioflavin-negative, synaptic-like deposits of PrP, as well as astrocytic gliosis; the cerebellum, hippocampus, and olfactory bulb are the regions of the brain most affected (4). We have now carried out a detailed chronological study of these features by immunohistochemical staining of brain sections with antibodies to PrP and to GFAP. Fig. 4 *H*–*J* and Table 2 show results for the cerebellum, but staining for PrP and GFAP is also consistently seen in the hippocampus and olfactory bulb. Fine punctate deposits of PrP in the molecular and granule cell layers are first visible by 30–40 days of age in Tg(PG14⁺/⁺) mice. Increased numbers and size of GFAP-positive astrocytes are evident in these two layers by 30 days of age, concomitant with an increase in the amount of GFAP protein in extracts of whole brain (Fig. 1*A*). Both of these pathological changes therefore significantly prefigure the appearance of clinical symptoms, which occurs in these animals at

64 days of age. PrP deposition and gliosis increase further during the symptomatic phase of the illness, although PrP immunostaining decreases in terminally ill mice (180 days old), probably as a result of substantial loss of granule cells which synthesize PrP. Neither thioflavin-positive plaques nor obvious spongiosis were observed at any time. No pathological changes were seen in Tg(WT-E1) or nontransgenic mice.

Discussion

Tg(PG14) mice model several key aspects of familial prion diseases in humans, including clinical symptoms, neuropathological changes, and the generation of PrP molecules with the biochemical features of PrP^{Sc} (4). These are currently the only genetically engineered mice that spontaneously produce a protease-resistant form of PrP, which is a hallmark of almost all infectious, sporadic, and familial cases of prion disease. Tg(PG14) mice are therefore valuable for addressing several important questions concerning the molecular pathogenesis of inherited prion disorders. Although only limited pathological and biochemical information is available on human patients that carry the PG14 mutation, more extensive studies have been carried out on patients with a six-octapeptide PrP insertion (21), and in a number of these cases features quite similar to those seen in Tg(PG14) mice have been described, including nonamyloid PrP deposition, lack of spongiosis, and depletion of cerebellar granule cells. Thus, it is very likely that the results we have obtained from our analysis of Tg(PG14) mice will be applicable to human patients with inherited prion diseases. Regardless of the exact correspondence between the phenotypes of our mice and those of human patients, however, our studies reveal several novel mechanistic insights into how a mutant form of PrP can cause neurodegeneration, including the role of the protease-resistant form of the protein in triggering the disease process, the cell death pathways that are activated, and the metabolism of the mutant protein in the brain.

Patients with familial prion diseases do not manifest symptoms until adulthood (2, 3), despite the fact that PrP is known to be expressed in the central nervous system beginning early in embryogenesis and to reach maximal levels soon after birth (22, 23). The question therefore arises of when during the lifetime of patients are mutant PrP molecules converted to the PrP^{Sc} state,

Fig. 5. DNA extracted from the cerebella of Tg(PG14) mice displays a 200-bp ladder. Detergent extracts of cerebella were centrifuged at 16,000 × g, and DNA extracted from pellet fraction (lanes 1, 3, 5, and 7) and supernatant fraction (lanes 2, 4, 6, and 8) was subjected to Southern blotting using restriction-digested mouse genomic DNA as a probe. Samples were from mice of the following ages: 182 days (lanes 1 and 2), 187 days (lanes 3 and 4), 178 days (lanes 5 and 6), and 176 days (lanes 7 and 8). One-thirtieth of the DNA extracted from the pellet fractions, and the whole amount of DNA extracted from the supernatant fractions were analyzed. Size markers are given in base-pairs.

and what role does PrP^{Sc} play in development of clinical illness? Is PrP^{Sc} produced beginning early in life or only in the adult? It has not been possible to address this question directly, since analysis of PrP^{Sc} in human subjects is of necessity restricted to a single time point at the terminal phase of the illness.

Our analysis of Tg(PG14) mice reveals that molecules with the biochemical properties of PrP^{Sc} accumulate throughout the life of the animal, but that neuropathological lesions and clinical disease do not ensue until a critical threshold level has been reached. In both Tg(PG14$^{+/+}$) and Tg(PG14$^{+/-}$) mice, detergent-insoluble and protease-resistant PrP are already detectable within the first week of life, long before clinical symptoms commence (at ≈65 and ≈240 days of age, respectively, in the two genotypes), and before the initiation of astrocytosis and granule cell apoptosis (at ≈30 days in both genotypes). PrP^{Sc} then accumulates in the brain as the mice age, reaching levels in terminally ill animals that are 20- to 80-fold higher than in newborn mice. This dramatic elevation of PrP^{Sc} is correlated with a marked astrocytic reaction and with progressive granule cell loss in the cerebellum. Of note, PrP^{Sc} increases more rapidly and reaches higher levels in Tg(PG14$^{+/+}$) than in Tg(PG14$^{+/-}$) mice (Fig. 2 C and D), correlating with the faster disease progression in homozygous animals. Taken together, these results argue strongly that PrP^{Sc} plays a primary pathogenic role in familial prion diseases, as it does in infectious forms, and is the causative factor in development of neuropathology and clinical symptoms. Our data also indicate that neurons at all stages of brain maturation possess the cellular and molecular machinery necessary for converting mutant PrP to a PrP^{Sc}-like state, and that this capability is not restricted to the adult nervous system.

Our results suggest that PG14 PrP accumulates in the brain because it turns over more slowly or is cleared less efficiently than WT PrP. The total amount of mutant PrP in the brains of Tg(PG14) mice increases ~10-fold during the life of the animal, whereas the amount of WT PrP in Tg(WT) and nontransgenic CD1 mice changes by <2-fold. Since levels of the mRNAs encoding mutant and WT PrP remain relatively constant after birth, the rates of synthesis of the two proteins are likely to be similar, assuming the absence of differential translational efficiency. Whether PG14 PrP is degraded more slowly within cells or whether it accumulates in a more stable form in the extracellular space of the brain remains to be determined. We have found that PG14 PrP has a slower metabolic half-life than WT PrP when expressed in transfected Chinese hamster ovary cells (24), but whether the same is true when the protein is expressed in neurons is not known.

Familial prion diseases exhibit considerable variability in their clinical and neuropathological presentation. A hypothesis to explain the anatomical specificity of each mutation is that neurons from different parts of the brain metabolize mutant PrPs in different ways, and that some populations of neurons convert particular mutant PrPs to the PrP^{Sc} state much more efficiently than other populations of neurons. Our analysis of Tg(PG14) mice indicates that this is not likely to be the case for the PG14 mutation. We find that PrP^{Sc} is widely distributed throughout the brains of both presymptomatic and terminally ill animals, as demonstrated by regional measurements of the amount of detergent-insoluble and protease-resistant PrP and by histoblotting of cryostat sections. Our results suggest that neurons in most parts of the brain are capable of converting PG14 PrP to a PrP^{Sc}-like state with similar efficiency. This conclusion is substantiated by studies of PrP^{Sc} formation in primary cultures of neurons derived from different brain regions of Tg(PG14) mice (B.D. and D.A.H., unpublished data). Moreover, the ability to produce PrP^{Sc}-like molecules does not seem to be restricted to neurons, since many peripheral tissues in Tg(PG14) mice also contain a protease-resistant and detergent-insoluble form of the mutant protein (R. C. and D. A. H., unpublished data). In addition, PG14 PrP acquires PrP^{Sc} properties in transfected Chinese hamster ovary cells in culture (24–26). The conclusion that
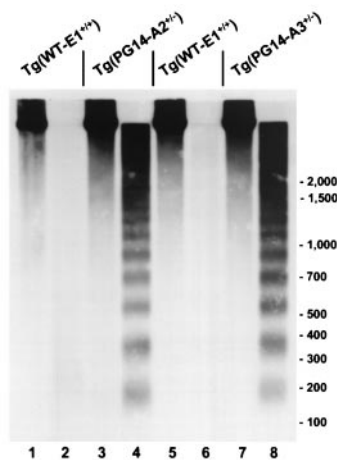
Chiesa *et al.*

emerges from these data is that the PG14 mutation structurally alters the protein in such a way that promotes conversion to the PrP^{Sc} state regardless of the cellular context. Other pathogenic mutations may operate in a more cell-specific fashion, for example, the FFI mutation which produces a more selective pattern of PrP^{Sc} accumulation (27).

The widespread anatomical distribution of PrP^{Sc} seen by Western blotting and histoblotting contrasts with the more restricted localization of punctate PrP deposits visible by immunohistochemical staining. These deposits are present mainly in the cerebellum, hippocampus, and olfactory bulb. This discrepancy could be attributable to anatomical variations in the physical state of PrP^{Sc}. For example, if PrP in the cerebellum and hippocampus was more aggregated than in other regions of the brain, then the protein there might have a greater resistance to the denaturing treatments (hydrolytic autoclaving and incubation with guanidine thiocyanate) applied before immunohistochemical staining.

A striking feature of Tg(PG14) mice is the degeneration of cerebellar granule cells. The consequent disruption of cerebellar circuitry is likely to contribute to the severe ataxia displayed by Tg(PG14) mice. Granule cells appear to be born in normal numbers, and they migrate to position in the internal granule cell layer in typical fashion. However, beginning within the first month of life, these cells undergo a degenerative process that displays the essential features of apoptosis, including nuclear condensation and fragmentation, ISEL-positive staining, internucleosomal cleavage of DNA, and caspase-3 activation. The depletion of granule cells appears to be relatively selective, since obvious neuronal loss is not visible in other areas of the brain. However, decreases in neuronal number are much easier to appreciate in densely populated regions such as the granule cell layer, so that changes in other areas cannot be ruled out. A careful examination of the other brain regions by ISEL will help to resolve this issue. Purkinje cells appear to be present in normal numbers in Tg(PG14) mice, although it must be kept in mind that the transgenic vector does not drive expression in this cell type

(28). Loss of granule cells has been seen in a number of cases of familial, sporadic, and infectious prion diseases (21, 29).

It is interesting to speculate on the cause of granule cell degeneration in Tg(PG14) mice. Since apoptosis is correlated with the accumulation of protease-resistant and detergent-insoluble PrP, a toxic effect of PrP^{Sc} may be responsible. If this is the case, however, granule cells must be particularly vulnerable to the toxic insult, since PrP^{Sc}-like molecules are present in many other parts of the brain that do not show obvious neuronal loss. Another factor contributing to granule cell apoptosis may be that PrP in the cerebellum is more toxic than in other brain regions, perhaps because the protein there is more highly aggregated, as suggested by the presence of the synaptic-like deposits visualized by immunohistochemical staining. A final possibility is that granule cells may be especially dependent on a normal physiological function of PrP^{C} which is compromised by the presence of the insertional mutation.

Although it is generally agreed that neuronal loss is a cardinal feature of prion diseases, the role of apoptosis in this process has received limited attention. A synthetic peptide derived from the PrP sequence causes apoptosis of cultured neurons (30). In addition, there have been several reports describing neuronal apoptosis in murine scrapie as well as in some cases of sporadic, familial, and iatrogenic Creutzfeldt-Jakob disease (31–34). In Tg(PG14) mice, granule cell apoptosis is a consistent and dramatic feature, thus providing a particularly clear-cut demonstration of the role of apoptosis in a prion disease. It will now be possible to use these mice to investigate the molecular triggers for the apoptotic process and to test therapeutic interventions.

1. Prusiner, S. B. (1998) *Proc. Natl. Acad. Sci. USA* **95,** 13363–13383.
2. Young, K., Piccardo, P., Dlouhy, S., Bugiani, O., Tagliavini, F. & Ghetti, B. (1999) in *Prions: Molecular and Cellular Biology*, ed. Harris, D. A. (Horizon Scientific Press, Wymondham), pp. 139–175.
3. Gambetti, P., Petersen, R. B., Parchi, P., Chen, S. G., Capellari, S., Goldfarb, L., Gabizon, R., Montagna, P., Lugaresi, E., Piccardo, P. & Ghetti, B. (1999) in *Prion Biology and Diseases*, ed. Prusiner, S. B. (Cold Spring Harbor Lab. Press, Cold Spring Harbor, NY), pp. 509–583.
4. Chiesa, R., Piccardo, P., Ghetti, B. & Harris, D. A. (1998) *Neuron* **21,** 1339–1351.
5. Owen, F., Poulter, M., Collinge, J., Leach, M., Lofthouse, R., Crow, T. J. & Harding, A. E. (1992) *Mol. Brain Res.* **13,** 155–157.
6. Duchen, L. W., Poulter, M. & Harding, A. E. (1993) *Brain* **116,** 555–567.
7. Krasemann, S., Zerr, I., Weber, T., Poser, S., Kretzschmar, H., Hunsmann, G. & Bodemer, W. (1995) *Mol. Brain Res.* **34,** 173–176.
8. Westaway, D., DeArmond, S. J., Cayetano-Canlas, J., Groth, D., Foster, D., Yang, S.-L., Torchia, M., Carlson, G. A. & Prusiner, S. B. (1994) *Cell* **76,** 117–129.
9. Muramoto, T., DeArmond, S. J., Scott, M., Telling, G. C., Cohen, F. E. & Prusiner, S. B. (1997) *Nat. Med.* **3,** 750–755.
10. Hegde, R. S., Mastrianni, J. A., Scott, M. R., Defea, K. A., Tremblay, P., Torchia, M., DeArmond, S. J., Prusiner, S. B. & Lingappa, V. R. (1998) *Science* **279,** 827–834.
11. Shmerling, D., Hegyi, I., Fischer, M., Blättler, T., Brandner, S., Götz, J., Rülicke, T., Flechsig, E., Cozzio, A., von Mering, C., *et al.* (1998) *Cell* **93,** 203–214.
12. Hsiao, K. K., Scott, M., Foster, D., Groth, D. F., DeArmond, S. J. & Prusiner, S. B. (1990) *Science* **250,** 1587–1590.
13. Telling, G. C., Haga, T., Torchia, M., Tremblay, P., DeArmond, S. J. & Prusiner, S. B. (1996) *Genes Dev.* **10,** 1736–1750.
14. Bolton, D. C., Seligman, S. J., Bablanian, G., Windsor, D., Scala, L. J., Kim, K. S., Chen, C. M., Kascsak, R. J. & Bendheim, P. E. (1991) *J. Virol.* **65,** 3667–3675.
15. Lehmann, S. & Harris, D. A. (1995) *J. Biol. Chem.* **270,** 24589–24597.
16. Taraboulos, A., Jendroska, K., Serban, D., Yang, S.-L., DeArmond, S. J. & Prusiner, S. B. (1992) *Proc. Natl. Acad. Sci. USA* **89,** 7620–7624.
17. Migheli, A., Piva, R., Wei, J., Attanasio, A., Casolino, S., Hodes, M. E., Dlouhy, S. R., Bayer, S. A. & Ghetti, B. (1997) *Am. J. Pathol.* **151,** 1629–1638.
18. Büeler, H., Fischer, M., Lang, Y., Fluethmann, H., Lipp, H.-P., DeArmond, S. J., Prusiner, S. B., Aguet, M. & Weissmann, C. (1992) *Nature (London)* **356,** 577–582.
19. Borchelt, D. R., Davis, J., Fischer, M., Lee, M. K., Slunt, H. H., Ratovitsky, T., Regard, J., Copeland, N. G., Jenkins, N. A., Sisodia, S. S., *et al.* (1996) *Genet. Anal. Biomol. Eng.* **13,** 159–163.
20. Wood, K. A., Dipasquale, B. & Youle, R. J. (1993) *Neuron* **11,** 621–632.
21. Collinge, J., Brown, J., Hardy, J., Mullan, M., Rossor, M. N., Baker, H., Crow, T. J., Lofthouse, R., Poulter, M., Ridley, R., *et al.* (1992) *Brain* **115,** 687–710.
22. Manson, J., West, J. D., Thomson, V., McBride, P., Kaufman, M. H. & Hope, J. (1992) *Development* **115,** 117–122.
23. McKinley, M. P., Hay, B., Lingappa, V. R., Lieberburg, I. & Prusiner, S. B. (1987) *Dev. Biol.* **121,** 105–110.
24. Lehmann, S. & Harris, D. A. (1996) *Proc. Natl. Acad. Sci. USA* **93,** 5610–5614.
25. Lehmann, S. & Harris, D. A. (1996) *J. Biol. Chem.* **271,** 1633–1637.
26. Daude, N., Lehmann, S. & Harris, D. A. (1997) *J. Biol. Chem.* **272,** 11604–11612.
27. Parchi, P., Castellani, R., Cortelli, P., Montagna, P., Chen, S. G., Petersen, R. B., Manetto, V., Vnencakjones, C. L., McLean, M. J., Sheller, J. R., *et al.* (1995) *Ann. Neurol.* **38,** 21–29.
28. Fischer, M., Rülicke, T., Raeber, A., Sailer, A., Moser, M., Oesch, B., Brandner, S., Aguzzi, A. & Weissmann, C. (1996) *EMBO J.* **15,** 1255–1264.
29. Parchi, P., Gambetti, P., Piccardo, P. & Ghetti, B. (1998) in *Progress in Pathology 4*, eds. Kirkham, N. & Lemoine, N. R. (Churchill Livingstone, Edinburgh), pp. 39–77.
30. Forloni, G., Angeretti, N., Chiesa, R., Monzani, E., Salmona, M., Bugiani, O. & Tagliavini, F. (1993) *Nature (London)* **362,** 543–546.
31. Dorandeu, A., Wingertsmann, L., Chrétien, F., Delisle, M.-B., Vital, C., Parchi, P., Montagna, P., Lugaresi, E., Ironside, J. W., Budka, H., *et al.* (1998) *Brain Pathol.* **8,** 531–537.
32. Giese, A., Groschup, M. H., Hess, B. & Kretzschmar, H. A. (1995) *Brain Pathol.* **5,** 213–221.
33. Lucassen, P. J., Williams, A., Chung, W. C. J. & Fraser, H. (1995) *Neurosci. Lett.* **198,** 185–188.
34. Gray, F., Chrétien, F., Adle-Biassette, H., Dorandeu, A., Ereau, T., Delisle, M.-B., Kopp, N., Ironside, J. W. & Vital, C. (1999) *J. Neuropathol. Exp. Neurol.* **58,** 321–328.

NEUROBIOLOGY